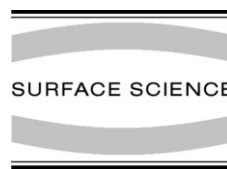




ELSEVIER

Surface Science 472 (2001) 89–96



www.elsevier.nl/locate/susc

C₆₀ adsorption on the quasicrystalline surface of Al₇₀Pd₂₁Mn₉

J. Ledieu^a, C.A. Muryn^b, G. Thornton^b, R.D. Diehl^c, T.A. Lograsso^d,
D.W. Delaney^d, R. McGrath^{e,*}

^a Surface Science Research Centre, The University of Liverpool, Liverpool L69 3BX, UK

^b Department of Chemistry, Manchester University, Manchester M13 9PL, UK

^c Department of Physics, Pennsylvania State University, University Park, PA 16802, USA

^d Ames Laboratory, Iowa State University, Ames, IA 50011, USA

^e Department of Physics, Surface Science Research Centre, The University of Liverpool, Liverpool L69 3BX, UK

Received 6 August 2000; accepted for publication 13 October 2000

Abstract

Room temperature adsorption of C₆₀ on the flat quasicrystalline surface of Al₇₀Pd₂₁Mn₉ has been investigated using scanning tunnelling microscopy. A dispersed overlayer is formed at low coverage, with avoidance of step-edges. There is no evidence of island formation or clustering. As the coverage is increased, a higher density layer is formed with no evidence of the formation of hexagonal ordered adsorbate structures seen on other substrates. This is followed by the onset of second layer formation. A range of bonding sites for C₆₀ molecules is implied from measurements of apparent molecular heights and from thermal effects. Detailed analysis of the surface at a low coverage (~0.065 ML) provides evidence of adsorbate local order, with Fibonacci (τ -scaling) relationships between the C₆₀ molecules. Where this occurs, the preferred adsorption site is tentatively identified as the pentagonal hollow. These local correlations however are not found to extend over larger regions of the surface. © 2001 Elsevier Science B.V. All rights reserved.

Keywords: Low energy electron diffraction (LEED); Scanning tunneling microscopy; Surface structure, morphology, roughness, and topography; Alloys

1. Introduction

Quasicrystal surfaces pose intriguing questions of both a fundamental and applied nature. It has been found that quasicrystals exhibit properties that may find technological applications in the near future; these include low surface energy, low friction and good corrosion resistance [1]. For a

comprehensive understanding of these properties, a detailed knowledge of the surface behaviour is a requirement. On the other hand, there are questions of a fundamental nature which also require answers. Under what conditions of preparation is the surface truly quasicrystalline? How does the geometry of the surface reflect that of the underlying bulk structure? Can current bulk models [2,3] be refined by the determination of the surface structure?

There has been an upsurge of activity to try and provide answers to these questions, and much of the attention of the surface community has

* Corresponding author. Tel.: +44-151-7943873; fax: +44-151-7080662.

E-mail address: r.mcgrath@liv.ac.uk (R. McGrath).

focussed on the icosahedral $\text{Al}_{70}\text{Pd}_{21}\text{Mn}_9$ quasicrystal. This is because it is possible to prepare large high quality single grains suitable for analysis using surface science techniques. In particular, scanning tunnelling microscopy (STM) has been applied to elucidate the quasicrystalline surface structure of this material [4–10]. Surfaces can be prepared in a highly perfect form with large (≥ 1500 Å) atomically flat terraces. We now know that it is Al-rich with a complex structure which is not known at the atomic scale [11–13], but with several repeating geometric features distributed across the surface with quasicrystalline ordering; in particular the surface has a dense distribution of five-fold pentagonal hollows of height 7 ± 1 Å¹ which display Fibonacci scaling relationships (also referred to as τ -scaling relationships, as the distances between hollows are non-periodic but proportional to the golden ratio $\tau = 1.618\dots$) [4–7].

A natural progression is to see how the geometry of the surface is modified when adsorbates are present. This is potentially important from a technological perspective; for example it may be possible to improve the friction properties by forming a thin molecular coating of a suitable molecule [14]. There is also the interesting possibility of whether a two-dimensional single species quasicrystalline overlayer can be formed. An atom or molecule adsorbing at a *unique* site on a quasicrystal surface could form such an overlayer by transference of the quasicrystallinity from the substrate ‘template’ to the adsorbate structure. Such overlayers would be very attractive for comparison with theoretical predictions of their expected symmetries [15], for study of a wide range of electronic and dynamic phenomena in two dimensions (2D) [16], and as physical realisations of the inflation property of Penrose tilings [17]. However, it is not obvious that such overlayers can be formed. Adsorbates such as oxygen [18] and sulphur [19] have been found to cause immediate disordering of this surface. This disordering may be due to their strong chemical bonds to the sur-

face atoms, leading to multiple-site and/or displacive adsorption.

To provide answers to some of the issues outlined above we choose C_{60} as a candidate adsorbate molecule. C_{60} has been shown to improve the frictional properties of surfaces [14]; furthermore it tends to stay intact upon adsorption and forms fairly weak bonds to the substrate. Its cage diameter (~ 7.1 Å) is of the same order as that of the pentagonal holes which decorate the quasicrystalline surface used in these studies. We have carried out extensive room temperature STM investigations of C_{60} adsorption on the five-fold surface of $\text{Al}_{70}\text{Pd}_{21}\text{Mn}_9$ combined with Auger electron spectroscopy (AES) and spot-profile analysis low energy electron diffraction (SPA-LEED) measurements. Here we report the results of these experiments and discuss the implications of our findings.

2. Experimental details

The $\text{Al}_{70}\text{Pd}_{21}\text{Mn}_9$ sample was cut perpendicular to its five-fold symmetrical axis and was polished using 6, 1 and 0.25 μm diamond paste on Texmet cloth for one hour. The initial measurements were carried out in an ultra-high vacuum (UHV) chamber equipped with an Omicron STM instrument and an Omicron LEED system that could also be used for retarding field AES. The dosing experiments were later repeated in a separate UHV chamber with an Omicron STM-1 instrument and a LEED optics. SPA-LEED measurements were conducted in a third chamber following the same surface preparation and using the same dosing system. The sample temperature was measured with an optical pyrometer in conjunction with a K-type thermocouple. The in-vacuum preparation of the sample consisted of cycles of sputtering at 1 keV by Ar^+ ions at a grazing angle for 90 min and annealing to 970 K for 2 h 30 min. The five-fold symmetric LEED patterns recorded after this treatment were very sharp with a very low background, and sample cleanliness was verified using AES. After such treatment the sample has large flat terraces and the detailed structure appears similar to that previously reported as quasicrys-

¹ This distance is measured from the centre of one side of the pentagon to the opposite apex.

talline by ourselves and other groups [4,8–10]. All STM images were taken with a positive sample bias which implies tunnelling into the unoccupied states of the surface.

The dosing system built to evaporate the C_{60} molecules (99.9 + % (HPLC)) consists of a tantalum wire tightly twisted around a glass tube. The temperature of the glass tube was measured by a K-type thermocouple placed at the level of the C_{60} molecules and the sample was at room temperature when dosing. The doser was at a temperature of 490 K which is high enough to evaporate C_{60} but does not cause cracking of the molecules. The doser was placed about 5 cm from the surface of the sample. AES was used to monitor the relative uptake of C_{60} as described in the next section, but because of difficulties in absolute coverage determination using AES, the amount of C_{60} was estimated by calculating the area covered by C_{60} molecules (based on their van der Waals diameter of 10 Å) as a fraction of the overall image area. This procedure allowed an approximate calibra-

tion of dosing time with coverage. All coverages quoted below are in monolayers (ML), and the error associated with coverage is estimated to be $\pm 20\%$ of the measurement. All measurements were taken at room temperature. The purity of the molecular flux was monitored by a mass spectrometer.

3. Results and discussion

Fig. 1 presents an overview of the adsorption behaviour. Fig. 1(a) is a $1000 \times 1000 \text{ Å}^2$ image of the clean surface after the preparation procedure described in the Section 2. Large terraces are present on the surface, which has a very small corrugation (typically $\leq 1 \text{ Å}$). Fig. 1(b) shows the surface with a coverage of 0.065 ML. The C_{60} molecules are clearly visible on the surface, consistent with other STM studies of this adsorbate [21]. At this coverage, the molecules form a dispersed layer, with no evidence for preferential

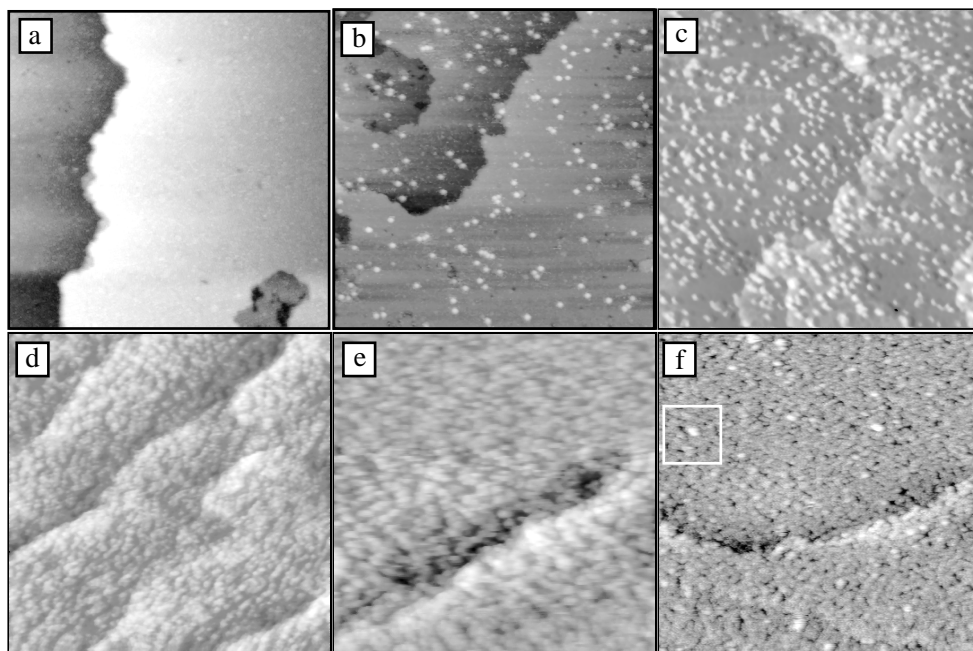


Fig. 1. (a) $1000 \times 1000 \text{ Å}^2$ STM image of the clean surface; (b) $1000 \times 1000 \text{ Å}^2$ STM image for 0.065 ML coverage (2.54 V, 1.04 nA); (c) $1000 \times 1000 \text{ Å}^2$ STM image for 0.13 ML coverage (0.59 V, 1 nA); (d) $1000 \times 1000 \text{ Å}^2$ for 0.26 ML coverage (0.93 V, 1 nA); (e) $900 \times 900 \text{ Å}^2$ for 0.54 ML coverage (0.98 V, 0.95 nA); (f) $900 \times 900 \text{ Å}^2$ for 1.05 ML coverage dosing (2 V, 0.95 nA). The white frame shows a $200 \times 200 \text{ Å}^2$ region which is analysed further in Fig. 5.

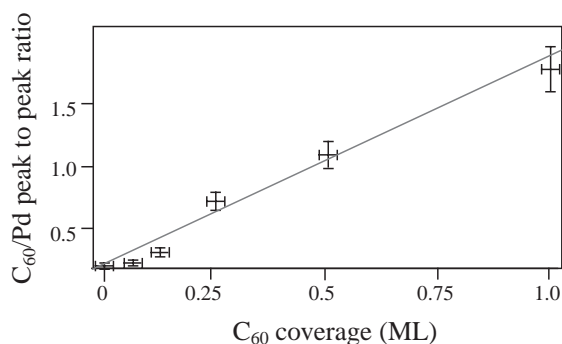


Fig. 2. Variation of the C₆₀/Pd peak to peak ratio as a function of coverage as determined by image analysis (as described in Section 2).

adsorption at the step-edges or of cluster or island formation. As the sample is further dosed the density of molecules increases in proportion to the dosing time Fig. 1(c)–(f). There is no evidence of the formation of hexagonal overlayers seen on other substrates, e.g. Al(1 1 1) [20]. AES scans were recorded for each of the coverages illustrated in Fig. 1. The ratio of the C_{KLL} peak to the Pd_{MNN} peak at 330 eV as a function of coverage as determined by image analysis. The results are shown in Fig. 2. This figure confirms an essentially linear uptake of C₆₀ molecules, consistent with the STM observations.

We now consider what information can be obtained on the bonding and orientation of the molecules from images of the molecules themselves. Fig. 3(a) shows a $100 \times 100 \text{ \AA}^2$ image of the surface with 0.065 ML coverage. The large apparent width of the C₆₀ molecules ($\geq 14 \text{ \AA}$) is typical of STM measurements of these molecules and is due to a tip apex-sample convolution [21]. (The van der Waals radius has been used to calculate the coverage as noted in Section 2 as the apparent diameter of the C₆₀ molecules is somewhat tip- and scan-dependent.) The clean surface areas between the C₆₀ molecules are not as well resolved as in a similar size scan of the clean surface, because of the presence of the C₆₀ molecules. Fig. 3(b) shows an $40 \times 40 \text{ \AA}^2$ region of the surface at the 1.05 ML coverage. Here the apparent molecular diameter is $10 \pm 2 \text{ \AA}$ (comparable to the van der Waals radius). At this coverage, the smaller apparent width of the molecules is presumably due to the smaller surface corrugation. In both Fig. 3(a) and (b) the molecules appear to display some internal structure, which may be an indication that they do not rotate on the surface [22,23]. However further work is needed to elucidate this point.

By measuring the apparent height of the molecules at low coverage, it was found that they group into three classes in almost equal numbers. Type A

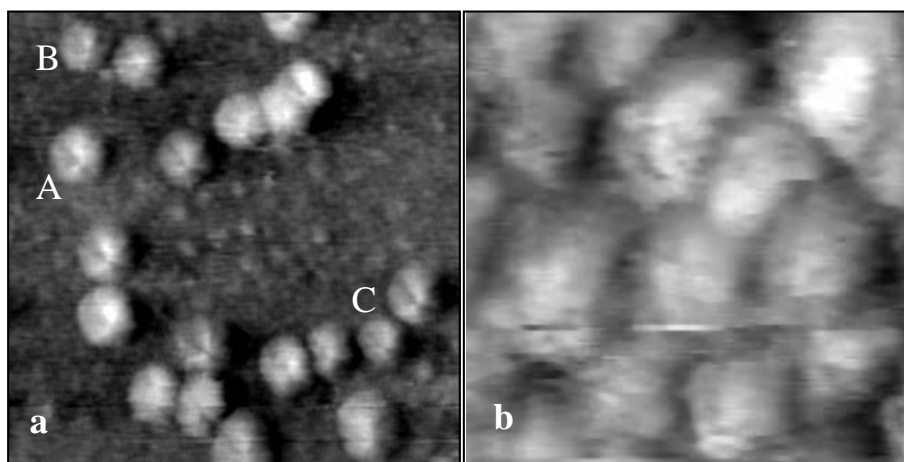


Fig. 3. (a) $150 \times 150 \text{ \AA}^2$ high Resolution STM image at a coverage of 0.065 ML (1.97 V, 1.04 nA). The molecules labelled A, B and C are discussed in the text. (b) $40 \times 40 \text{ \AA}^2$ region of the surface for a coverage of 1.05 ML (0.5 V, 0.95 nA).

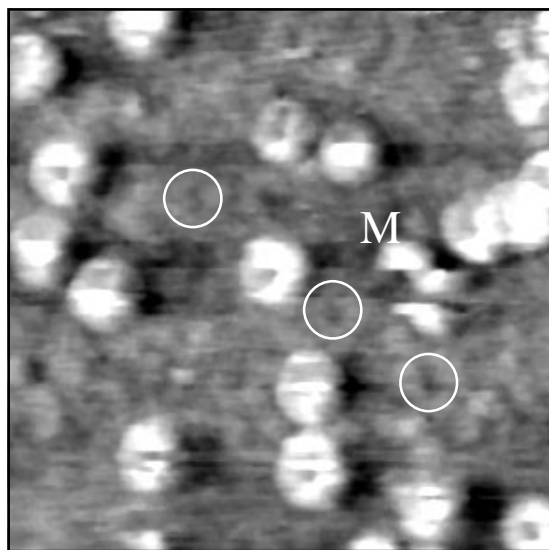


Fig. 4. $150 \times 150 \text{ Å}^2$ STM image of the flat $\text{Al}_{70}\text{Pd}_{21}\text{Mn}_9$ surface at a coverage of 0.065 ML (1.97 V, 1.04 nA). The molecule marked M is diffusing across the surface, under the influence of the STM tip. The circles denote the five-fold hollows discussed further in relation to Fig. 7.

has an apparent height above the surface of $7.6 \pm 1 \text{ Å}$, type B a height of $6.3 \pm 1 \text{ Å}$, and type C a height of $5.6 \pm 1 \text{ Å}$. The presence of three distinct heights of molecules at low coverage is an indication of different bonding sites on the surface. The height difference has two possible origins: a topographical contribution due to bonding in hollows of different depths, and the possibility of bonding to different atomic species in the surface. (A small apparent height can correspond to a re-

duction in the local density of states of the C_{60} due to a stronger interaction with the substrate [22].) The most likely explanation is a combination of these effects, as due to the complexity of the surface, different hollows on the surface will have different atomic environments also [11,12].

We have also observed tip-induced motion of molecules on the surface. Fig. 4 shows a $150 \times 150 \text{ Å}^2$ section of the surface at the 6.5% C_{60} coverage. An example of such a motion taking place is shown in Fig. 4. This indicates that the molecule experiences a fairly flat potential energy profile as it moves across the surface and is not necessarily an indication of a weak bonding strength. Evidence that some of the molecules are more weakly bonded than others comes from heating the sample. When the monolayer surface represented in Fig. 1(f) is annealed to 600 K, partial desorption of the molecules results leaving a surface which has a coverage of about 0.25 ML as measured with AES. Overall, the picture which emerges is that C_{60} occupies a range of bonding sites on this surface.

At the 1.05 ML coverage the start of second layer growth is observed. The surface at this stage is almost covered with C_{60} molecules, but it is still possible to find some areas of the surface which are not saturated. Fig. 5(a) is a larger scale image of the framed region of Fig. 1(f). The white line indicates the direction of the line profile shown in Fig. 5(b). The height difference between the bottom of the trough and the peak of the protrusion is measured at $13.9 \pm 1 \text{ Å}$. This is close to twice the C_{60} cage diameter (7.1 Å) and indicates that the protrusion represents a molecule in the second

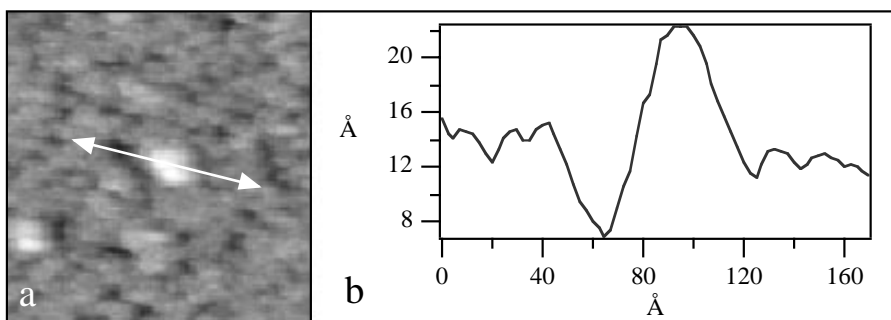


Fig. 5. (a) $200 \times 200 \text{ Å}^2$ region framed on Fig. 1(f) for 1.05 ML coverage (2 V, 0.95 nA) and (b) plot profile of the line present on (a). The height difference is $13.9 \pm 1 \text{ Å}$ which corresponds to twice a C_{60} molecule height.

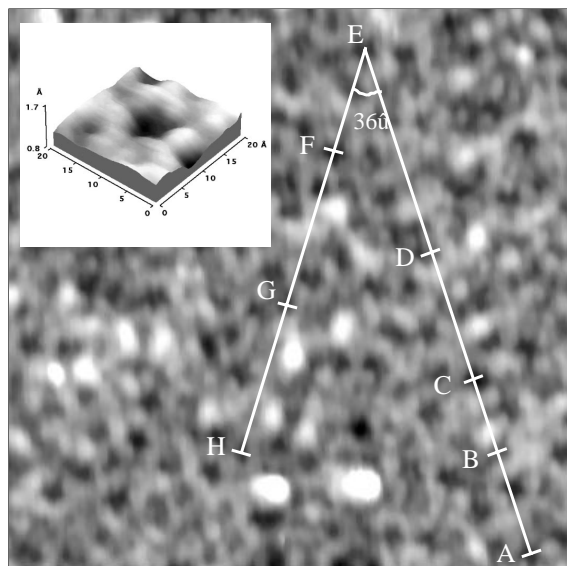


Fig. 6. $150 \times 150 \text{ \AA}^2$ STM image of the flat $\text{Al}_{70}\text{Pd}_{21}\text{Mn}_9$ surface (1.97 V, 1.04 nA). Sequences of pentagonal hollows labelled A, B, ..., H along two directions are indicated. The angle between these two lines is present in a Fibonacci pentagrid. Inset: a close-up view of one of the pentagonal hollows.

layer. Several other such molecules are visible in Fig. 1(f).

We now consider whether the molecules display any symmetry interrelationships. The LEED pattern from the surface is still visible for the 0.54 ML coverage although SPA-LEED measurements at this coverage indicate that the intensity is reduced by $\sim 50\%$. The pattern disappears completely at the 1.05 ML coverage. This corresponds to the completion of the first layer of C_{60} molecules. However the molecules themselves do not appear to adopt any special symmetry relationships. Fast Fourier transforms (FFTs) were carried out for each of the images, and a five-fold pattern was observed only for the lowest coverage studied (0.065 ML), which is probably due to the underlying surface structure. Another way of characterising the symmetry relationships between objects which do not exhibit translational symmetry is through the use of 2D autocorrelation patterns of the images. This technique has been used to good effect to provide quantitative information on the distribution of features visible in high resolution images of the clean surface of the $\text{Al}_{70}\text{Pd}_{21}\text{Mn}_9$

quasicrystal [4,10]. However the autocorrelations of the C_{60} molecules in Fig. 1(b)–(f) do not show any evidence of long-scale ordering of the molecules. These results indicate that the LEED pattern observed from the surface as dosed in Fig. 1(b)–(e) is due to the residual part of the surface which is not covered by C_{60} molecules.

The lack of symmetry observed and indeed the apparent existence different bonding arrangements at low coverage (A, B and C in Fig. 3(a)) rule out the possibility of long-range correlations between the C_{60} molecules on the surface. This does not however exclude local ordering of C_{60} molecules. In Fig. 6 we present a $150 \times 150 \text{ \AA}^2$ image of a terrace of the clean surface after the preparation procedures described above. A feature intrinsic to this surface is the distribution of large protrusions which appear as the bright features in the images. These large protrusions appear to be defects on the surface, and their density can be reduced by refinement of the preparation procedure. Another feature of this surface is a dense distribution of pentagonal hollows, several of which are marked in Fig. 6. Such pentagonal hollows appear in the model of Gierer et al. [12]; they do not all have the same atomic composition. A higher magnification $20 \times 20 \text{ \AA}^2$ image of one of these hollows is shown as an inset in this figure. Schaub and coworkers have shown that these pentagonal hollows are aligned along a Fibonacci pentagrid on the surface [4–7]. This means that successive spacings of planes of these hollows have either long (L) or short (S) interplanar spacings, with the ratio of L to S being τ , the golden ratio [24].² The distances between such hollows are subject to τ -scaling relationships: if the distance between two hollows on a line is multiplied by the golden ratio τ or multiples of τ then the resulting distance locates other such hollows along the same line. The minimum separation between the centres of such hollows is about 12 Å. All hollows on the surface have such scaling interrelationships; some examples (chosen

² The Fibonacci sequence consists of terms such that the n th term is the sum of the $n-1$ and $n-2$ terms; furthermore the ratio of successive terms approaches the golden ratio τ as n becomes large; τ is an irrational number whose first few terms are $\tau = 1.618 \dots$

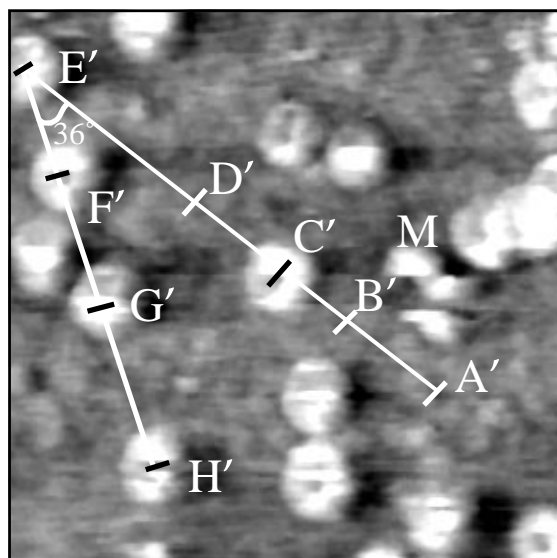


Fig. 7. $150 \times 150 \text{ \AA}^2$ STM image of the flat $\text{Al}_{70}\text{Pd}_{21}\text{Mn}_9$ surface at a coverage of 6.5% (1.97 V, 1.04 nA). C_{60} molecules adsorb on the pentagonal hollows, leading to τ -scaling relationships between the molecules as described in the text.

specifically with the following discussion of C_{60} adsorption in mind) are shown in Fig. 6; the distances $[\text{AB}] = 30 \pm 3 \text{ \AA}$, $[\text{AC}] = 50 \pm 3 \text{ \AA}$, $[\text{AD}] = 85 \pm 4 \text{ \AA}$ and $[\text{AE}] = 141 \pm 5 \text{ \AA}$. Thus within experimental error

$$[\text{AE}] = \tau[\text{AD}] = \tau^2[\text{AC}] = \tau^3[\text{AB}] \quad (1)$$

and similarly

$$[\text{EH}] = \tau[\text{EG}] = \tau^3[\text{EF}]. \quad (2)$$

We now demonstrate that *local* ordering can occur on the surface. Fig. 7 shows a $150 \times 150 \text{ \AA}^2$ section of the surface at the 0.065 ML C_{60} coverage (this image is identical to that in Fig. 4). It is possible to locate some of the unoccupied five-fold pentagonal hollows; these are shown encircled in Fig. 4 and are marked with dashes in Fig. 7. The positions of several C_{60} molecules are marked as C' , E' , F' , G' and H' . The distances between the holes labelled A' , B' and D' , are the same as for A , B and D on the clean surface in Fig. 6; it can be implied that the C_{60} molecules adsorbed in the positions C' , E' , F' , G' and H' are directly on-top of the underlying hollows. The correspondence

between the distances measured in the two figures leads us to tentatively assign the adsorption site as the pentagonal hollow for these molecules. The τ -scaling relationships found in Fig. 6 are transferred to the C_{60} molecules; for example Eqs. (1) and (2) apply now to the C_{60} molecules in the form:

$$[\text{A}'\text{E}'] = \tau[\text{A}'\text{D}'] = \tau^2[\text{A}'\text{C}'] = \tau^3[\text{A}'\text{B}'] \quad (3)$$

and

$$[\text{E}'\text{H}'] = \tau[\text{E}'\text{G}'] = \tau^3[\text{E}'\text{F}'] \quad (4)$$

Thus for these molecules, the surface acts as a template for quasicrystalline adsorption. Note that these molecules are not necessarily of the same type as defined above; this suggests that the different types observed could be related to C_{60} adsorption in hollows of different types. If it were possible to occupy all of the pentagonal hollow sites on the surface and no others this would constitute a two-dimensional inflated quasicrystalline overlayer; this would be a single species physical realization of the inflation property pointed out originally by Penrose [18]. This might be achievable by either careful dosing calibration or by controlled annealing of a saturated C_{60} monolayer; however our attempts to do so in this work were not successful.

4. Conclusions

We have characterised the deposition of C_{60} molecules on the quasicrystalline AlPdMn surface using STM, AES and SPA-LEED. The molecules adsorb randomly on the surface, forming dispersed layers of increasing density as the coverage is increased. The onset of second layer formation has been observed. The C_{60} molecules have a range of bonding sites on this surface, and some can undergo tip-induced movements. Local τ -scaling relationships between molecules were identified with bonding of these molecules in five-fold hollow sites. However it was not possible to form a 2D quasicrystalline overlayer.

Acknowledgements

The EPSRC (grant numbers GR/N18680 and GR/N25718) and NFS (grant number DMR-9817977) are acknowledged for funding. S.D. Barrett is thanked for guidance in the use of his analysis program ImageSXM (see <http://reg.ssci.liv.ac.uk/>).

References

- [1] J.M. Dubois, *Physica Scripta* T 49A (1993) 17.
- [2] M. Boudard, M. de Boisseau, *Physical Properties of Quasicrystals*, Springer Series in Solid State Sciences, Springer, Berlin, 1999, pp. 91–126.
- [3] G. Kasner, Z. Papadopolos, P. Kramer, D.E. Bürgler, *Phys. Rev. B* 60 (1999) 3899.
- [4] T.M. Schaub, D.E. Bürgler, H.-J. Güntherodt, J.-B. Suck, *Phys. Rev. Lett.* 73 (1994) 1255.
- [5] T.M. Schaub, D.E. Bürgler, H.-J. Güntherodt, J.-B. Suck, *Z. Phys. B* 96 (1994) 93.
- [6] T.M. Schaub, D.E. Bürgler, H.-J. Güntherodt, J.B. Suck, M. Audier, *Appl. Phys. A* 61 (1995) 491.
- [7] T.M. Schaub, D.E. Bürgler, C.M. Schmidt, H.-J. Güntherodt, *J. Non-Cryst. Solids* 205/207 (1996) 748.
- [8] J. Ledieu, A.W. Munz, T.M. Parker, R. McGrath, R.D. Diehl, D.W. Delaney, T.A. Lograsso, *Surf. Sci.* 433/435 (1999) 666.
- [9] J. Ledieu, A.W. Munz, T.M. Parker, R. McGrath, R.D. Diehl, D.W. Delaney, T.A. Lograsso, *Mat. Res. Soc. Symp. Proc.* 553 (1999) 237.
- [10] Z. Shen, C.R. Stoldt, C.J. Jenks, T.A. Lograsso, P.A. Thiel, *Phys. Rev. B* 60 (1999) 14688.
- [11] M. Gierer, M.A. Van Hove, A.I. Goldman, S.-L. Chang, W.Z. Shen, C.-M. Zhang, C.J. Jenks, P.A. Thiel, *Phys. Rev. Lett.* 78 (1997) 467.
- [12] M. Gierer, M.A. Van Hove, A.I. Goldman, Z. Shen, S.-L. Chang, P.J. Pinhero, C.J. Jenks, J.W. Anderegg, C.-M. Zhang, P.A. Thiel, *Phys. Rev. B* 57 (1998) 7628.
- [13] C.J. Jenks, T.A. Lograsso, P.A. Thiel, *J. Am. Chem. Soc.* 120 (1998) 12668.
- [14] W. Allers, C. Hahn, M. Lohndorf, S. Lukas, S. Pan, U.D. Schwarz, R. Wiesendanger, *Nanotechnology* 7 (1996) 346.
- [15] R. Lifshitz, *Physica A* 232 (1996) 633.
- [16] A. Zangwill, *Physics at Surfaces*, CUP, Cambridge, 1988.
- [17] R. Penrose, *Bull. Inst. Math. Appl.* 10 (1974) 266.
- [18] S.-L. Chang, W.B. Chin, C.-M. Zhang, C.J. Jenks, P.A. Thiel, *Surf. Sci.* 337 (1995) 135.
- [19] J.S. Ko, A.J. Gellman, T.A. Lograsso, C.J. Jenks, P.A. Thiel, *Surf. Sci.* 423 (1999) 243.
- [20] M.K.-J. Johansson, A.J. Maxwell, S.M. Gray, P.A. Brühwiler, D.C. Mancini, L.S.O. Johansson, N. Mårtensson, *Phys. Rev. B* 54 (1996) 13472.
- [21] X. Yao, T.G. Ruskell, R.K. Workman, D. Sarid, D. Chen, *Surf. Sci.* 367 (1996) L85.
- [22] X. Yao, R.K. Workman, C.A. Peterson, D. Chen, D. Sarid, *Appl. Phys. A* 66 (1998) S107.
- [23] A. Kasuya, C.-W. Hu, K. Tohji, T. Takahashi, Y. Nishina, *Appl. Phys. A* 66 (1998) 1279.
- [24] R.A. Dunlop, *The Golden Ratio and Fibonacci Numbers*, World Scientific, Singapore, 1997.